Cytoplasmic protein methylation is essential for neural crest migration

Katie L. Vermillion, Kevin A. Lidberg, and Laura S. Gammill

Department of Genetics, Cell Biology, and Development, University of Minnesota, Minneapolis, MN 55455

As they initiate migration in vertebrate embryos, neural crest cells are enriched for methylation cycle enzymes, including S-adenosylhomocysteine hydrolase (SAHH), the only known enzyme to hydrolyze the feedback inhibitor of trans-methylation reactions. The importance of methylation in neural crest migration is unknown. Here, we show that SAHH is required for emigration of polarized neural crest cells, indicating that methylation is essential for neural crest migration. Although nuclear histone methylation regulates neural crest gene expression, SAHH and lysine-methylated proteins are abundant in the cytoplasm of migratory neural crest cells. Proteomic profiling of cytoplasmic, lysine-methylated proteins from migratory neural crest cells identified 182 proteins, several of which are cytoskeleton related. A methylation-resistant form of one of these proteins, the actin-binding protein elongation factor 1 alpha 1 (EF1α1), blocks neural crest migration. Altogether, these data reveal a novel and essential role for post-translational non-histone protein methylation during neural crest migration and define a previously unknown requirement for EF1α1 methylation in migration.

Introduction

Neural crest cells migrate throughout vertebrate embryos using stereotyped behaviors (Kulesa and Gammill, 2010). After neural crest cells undergo an epithelial-to-mesenchymal transition to emigrate from the neural tube, they extend lamellipodia and filopodia to contact their neighbors and form chain arrangements (Kulesa and Fraser, 2000; Teddy and Kulesa, 2004; Berndt et al., 2008). Complement component 3a–mediated co-attraction allows these formations to move collectively, while environmental cues stabilize N-cadherin–dependent cell–cell contacts in a polarized manner to promote their directionality (Theveneau and Mayor, 2010; Carmona-Fontaine et al., 2011). Inside the cell, noncanonical Wnt signaling orients neural crest cell protrusive activity through effects on Rho GTPases that coordinate actin cytoskeletal remodeling (De Calisto et al., 2005; Matthews et al., 2008; Clay and Halloran, 2011; Theveneau and Mayor, 2012). Nevertheless, based upon analysis of other migratory cell types, we still have much to learn about neural crest cell migration.

Post-translational modifications regulate protein activity and interactions to affect actin polymerization and cell adhesion in migrating cells (Ammer and Weed, 2008; Rottner and Stradal, 2011; Boulter et al., 2012; Schaefer et al., 2012). For example, signaling through Rho GTPases and the activity of their targets is regulated post-translationally (Boulter et al., 2012). In fact, the phosphorylation status of a downstream target of Rho GTPases, the actin-depolymerizing factor cofilin, regulates neural crest cell directional migration (Y. Zhang et al., 2012). In spite of this, the post-translational control of neural crest migration has been largely ignored.

Just before migration, enzymes of the core methylation cycle are enriched in neural crest cells, suggesting that methylation regulates early neural crest development (Gammill and Bronner-Fraser, 2002; Adams et al., 2008). Indeed, in order for neural crest specification to proceed, the DNA methyltransferase DNMT3A must silence expression of *Sox2* and *Sox3* that drive neural fate (Hu et al., 2012). In addition, removal of repressive (Strobl-Mazzulla et al., 2010) and addition of activating histone methylation (unpublished data) are required for spatiotemporal regulation of neural crest gene expression that specifies neural crest cell identity (Bajpai et al., 2010; Prasad et al., 2012). Although neural crest cells with methylation-dependent

THE JOURNAL OF CELL BIOLOGY

specification defects also fail to migrate, it has been difficult to distinguish a role for methylation during neural crest migration from indirect effects of failed specification. Moreover, as methylation also has transcriptional, post-transcriptional, and post-translational consequences for cell function (Dricu, 2012), nonepigenetic roles for methylation in the neural crest await discovery.

Lysine methylation of nonhistone proteins modulates their stability (e.g., p53 [Chuikov et al., 2004]), localization (e.g., SF2/ASF [Sinha et al., 2010]; HSP70 [Cho et al., 2012]), protein–protein interactions (e.g., BRCA1 [Guendel et al., 2010]), and/or enzymatic activities (e.g., RIP140 [Huang and Berger, 2008; Huq et al., 2009; X. Zhang et al., 2012]). There is also evidence to suggest that nonhistone protein methylation regulates cell migration. For example, *S*-adenosylhomocysteine hydrolase (SAHH), which breaks down the feedback inhibitor of methylation reactions and is essential for further methylation reactions to proceed, redistributes to the leading edge of motile, chemotaxing *Dictyostelium* and is necessary to maintain cell polarity that drives chemotaxis (Shu et al., 2006). Meanwhile, Slit-Robo GTPase-activating protein 2 (srGAP2), which promotes protrusive activity to negatively regulate neuronal cell migration, must be arginine methylated for localization into protrusions (Guerrier et al., 2009; Guo and Bao, 2010). In addition, the lysine methyltransferase, enhancer of zeste homologue 2 (Ezh2), is cytoplasmically required for actin polymerization during fibroblast membrane ruffling (Su et al., 2005), and valosin-containing protein lysine methyltransferase is required for invasive cell migratory behaviors in cultured human cells (Kernstock et al., 2012). Moreover, nonhistone protein methylation is essential for bacterial chemotaxis and *Toxoplasma* parasite motility (Vladimirov and Sourjik, 2009; Heaslip et al., 2011). Nevertheless, the specific nonhistone proteins that are methylated in migratory eukaryotic cells, as well as the possibility that nonhistone protein methylation regulates neural crest migration, have not been investigated.

Here, we analyze the role of methylation in neural crest migration. Chick neural crest cells express SAHH mRNA and protein, and SAHH is required for the emigration of polarized migratory neural crest cells, suggesting that methylation is essential for neural crest migration. In contrast with the established role of nuclear histone methylation in neural crest gene expression (Bajpai et al., 2010; Strobl-Mazzulla et al., 2010; and unpublished data), SAHH and lysine-methylated proteins are abundantly cytoplasmic in migratory neural crest cells. This led us to postulate that cytoplasmic protein methylation regulates the dynamic process of neural crest migration. We profiled cytoplasmic proteins with mono- and dimethylated lysines in migratory neural crest cells, identifying a number of cytoskeleton-associated factors. To test the functional relevance of this methylation during neural crest migration, we focused on one target in particular, elongation factor 1-α 1 (EF1α1), which binds actin filaments and β-actin mRNA to localize actin translation to the leading edge of migratory cells (Liu et al., 2002; Condeelis and Singer, 2005). Mutating the methylated lysines in EF1α1 inhibits neural crest migration. This is, to our knowledge, the first function to be ascribed to EF1α1 methylation. Altogether, our work defines the novel requirement for methylation during neural crest migration, and specifically reveals the importance of nonhistone lysine methylation in migratory neural crest cells.

Results

Neural crest cells express SAHH

Gene expression profiling of neural crest cells identified several enzymes that regulate methylation reactions, including SAHH (Gammill and Bronner-Fraser, 2002; Adams et al., 2008). SAHH hydrolyzes *S*-adenosylhomocysteine (SAH), which is a byproduct of trans-methylation reactions and a potent methyltransferase inhibitor (Fig. S1 A; Chiang et al., 1996). *SAHH* mRNA was broadly expressed at varying levels throughout early chicken embryos, but was particularly abundant in premigratory neural crest precursors in the neural folds of cranial, hindbrain, and trunk domains (Fig. S1, B–E and I, white arrowheads), as well as in the nonneural ectoderm (Fig. S1, C and G, black arrows; nne). *SAHH* expression persisted in HNK-1–positive (Fig. S1 G′, white arrow) cranial migratory neural crest cells (Fig. S1, F–H, black arrowheads). The robust expression of *SAHH* in neural crest cells suggests that methylation is important for early stages of neural crest development.

SAHH is required for neural crest migration

Because SAHH is essential to clear the methyltransferase feedback inhibitor SAH, one way to prevent methylation is to block SAHH (Fig. S1 A; Fabianowska-Majewska et al., 1994). We first examined the requirement for SAHH during neural crest migration in vivo using a translation-blocking antisense morpholino oligonucleotide (SAHH MO). We unilaterally targeted SAHH MO into neural crest precursors by electroporation at late gastrula, at the time of neural crest induction (Basch et al., 2006; Gammill and Krull, 2011). This allowed SAHH, which is a stable protein (Ueland and Helland, 1983), sufficient time to turn over in targeted cells. After incubation for 8 or 14 h to 4 or 8 somites, cells targeted with fluorescein-modified SAHH MO exhibited reduced or absent SAHH immunofluorescence, indicating that the MO effectively knocked down SAHH protein (Fig. S2, A′′ and B′′, circles).

Although we were interested in migration, sustained SAHH knockdown could also affect specification once sufficient time elapsed for SAH to accumulate and inhibit methyltransferase activity. In particular, DNA methyltransferase 3A (DNMT3A) and the lysine methyltransferase, nuclear SET-domain containing protein 3 (NSD3), are required for neural crest specification (Hu et al., 2012; unpublished data). To gain temporal insight, we evaluated two key neural crest transcription factors: *Snail2*, a target of neural plate border specifiers, and *Sox10*, a downstream target of other neural crest transcription factors (Prasad et al., 2012). Expression of *Snail2* (Fig. 1, A–C) and *Sox10* (Fig. 1, D–F) was scored in SAHH MO–targeted (white arrowhead) compared with untargeted (black arrowhead) sides of electroporated embryos with 4–6 somites in regions of maximal MO targeting. Relative to control MO–electroporated embryos (CO MO), *Snail2* expression was minimally altered in SAHH MO–electroporated embryos (Fig. 1 B, white arrowhead;
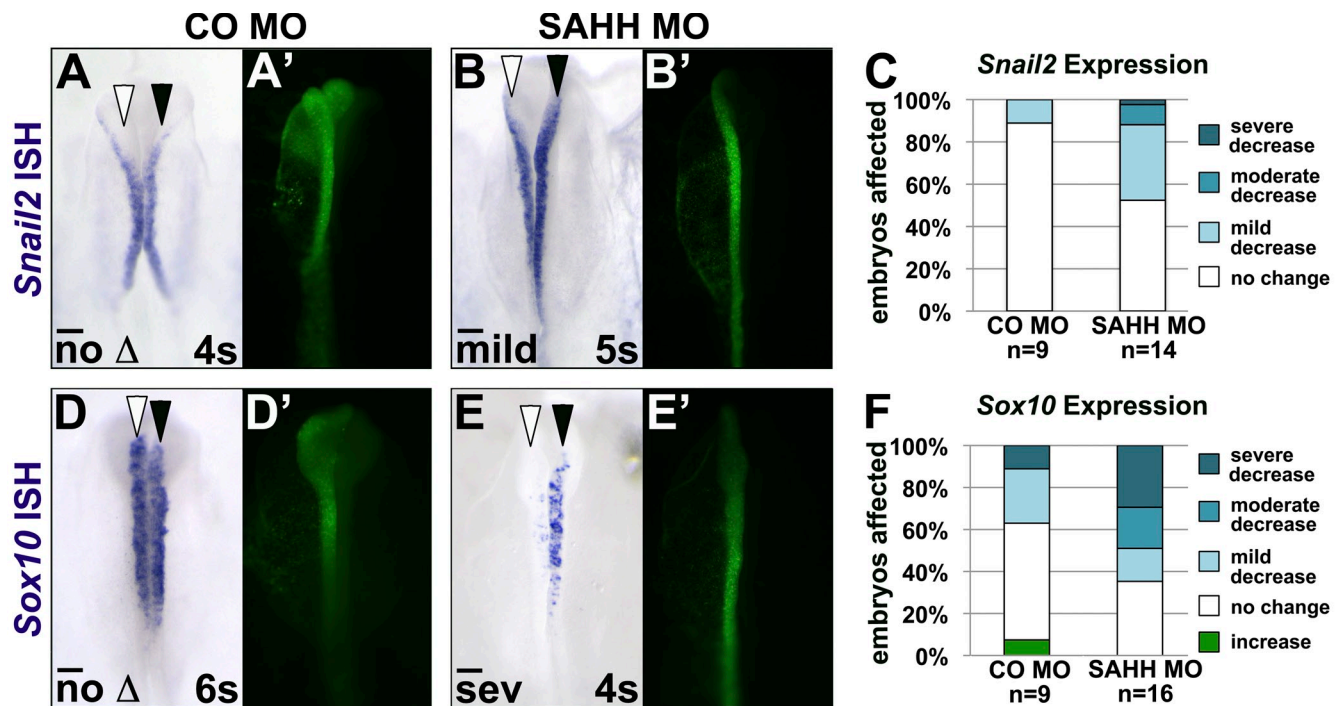
Figure 1. SAHH is required for neural crest cell specification. Embryos were unilaterally electroporated with standard control MO (CO MO; A′ and D′, green) or SAHH MO (B′ and E′, green) at late gastrula, reincubated to 4–6 somites (s), and processed by in situ hybridization (purple) to visualize expression of *Snail2* (A and B) or *Sox10* (D and E). White arrowhead, targeted side of embryo; black arrowhead, untargeted side of embryo. (A and B) *Snail2* expression is mildly affected on the SAHH MO–targeted side (representative example shown in B; P = 0.07). (C) Stacked bar graph depicting the frequency and severity of *Snail2* expression defects in embryos electroporated with CO MO or SAHH MO. (D and E) *Sox10* expression is severely altered on the SAHH MO–targeted side (representative example shown in E; P = 3.44×10^{-3}). (F) Stacked bar graph depicting the frequency and severity of *Sox10* expression defects in embryos electroporated with CO MO or SAHH MO. (A, B, D, and E) dorsal views, fluorescent MO targeting in right panel. Bars, 100 µm.

Fig. 1 C, P = 0.07). In contrast, the *Sox10* expression domain was mildly to severely reduced in the majority of the SAHH MO–electroporated embryos (Fig. 1 E, white arrowhead; Fig. 1 F, P = 3.44×10^{-3}; phenotype examples in Fig. S3). Thus, methyl-transferases became inhibited during neural crest specification in SAHH MO–electroporated embryos.

Next, we determined the impact of SAHH knockdown on neural crest migration. First, we examined the distance migrated by the *Sox10*-expressing cells that formed on the SAHH MO–targeted side compared with the untargeted side at 8–10 somites (Fig. 2, A–C). SAHH MO–targeted neural crest cells exhibited mildly to severely reduced neural crest migration (Fig. 2 B, white arrowhead; Fig. 2 C, P = 2.05×10^{-4}; phenotype examples in Fig. S3). As *Sox10* expression was affected by SAHH knockdown (Fig. 1 E), we also assayed the general migratory neural crest cell marker, HNK-1, and found that migration of HNK-1–positive cells was similarly reduced (Fig. 2 E, white arrowhead; Fig. 2 F, P = 0.04). Reduced migration was not a result of increased cell death or decreased proliferation (Fig. S2, D–G). Moreover, this phenotype could be rescued by adding back SAHH (Fig. S4). Altogether, these data support a requirement for methylation during neural crest cell specification, and suggest that SAHH, and thus methylation, are crucial for neural crest migration. However, sustained knockdown does not distinguish whether migration is disrupted as an indirect consequence of defective specification, or due to a direct requirement for SAHH during migration.

To block SAHH activity specifically during neural crest migration, we treated neural crest cultures with the efficient SAHH inhibitor tubercidin, or 7-deaza-adenosine (Fig. S1 A; Fabianowska-Majewska et al., 1994). After 16–24 h of culture, carrier-treated neural tube explants showed characteristic migration of HNK-1–positive neural crest cells (Fig. 3 A, white arrowheads) in large numbers (Fig. 3 D) at a distance around the neural tube (Fig. 3 C). In contrast, neural tube explants incubated in 1.0 µM tubercidin produced fewer HNK-1–positive migratory neural crest cells (Fig. 3, B [white arrowhead] and D) that traveled shorter distances away from the neural tube (Fig. 3 C). Interestingly, tubercidin-treated neural crest cells extended processes in all directions (Fig. 3 B′) whereas carrier-treated migratory neural crest cells exhibited polarized protrusions (Fig. 3 A′). Indeed, length/width ratios of tubercidin-treated cells were significantly reduced and closer to 1 (symmetrical) compared with control-treated cells (Fig. 3 E). Inhibition of migration was tubercidin dose dependent, indicating specificity (Fig. S2, H–K). Moreover, tubercidin treatment did not increase cell death in the explants (Fig. S2 L), and tubercidin-treated cells extended protrusions over the full 16–24-h time course of the experiment. This suggests that these effects were not due to inhibition of the alternate tubercidin target, adenosine deaminase, as blocking this enzyme is toxic to cells (Hershfield and Krodich, 1978; Kozlowska et al., 1999). Altogether, these results indicate that neural crest cell emigration, migration, and polarization require SAHH, and thus methylation, independent of its role during neural crest specification.
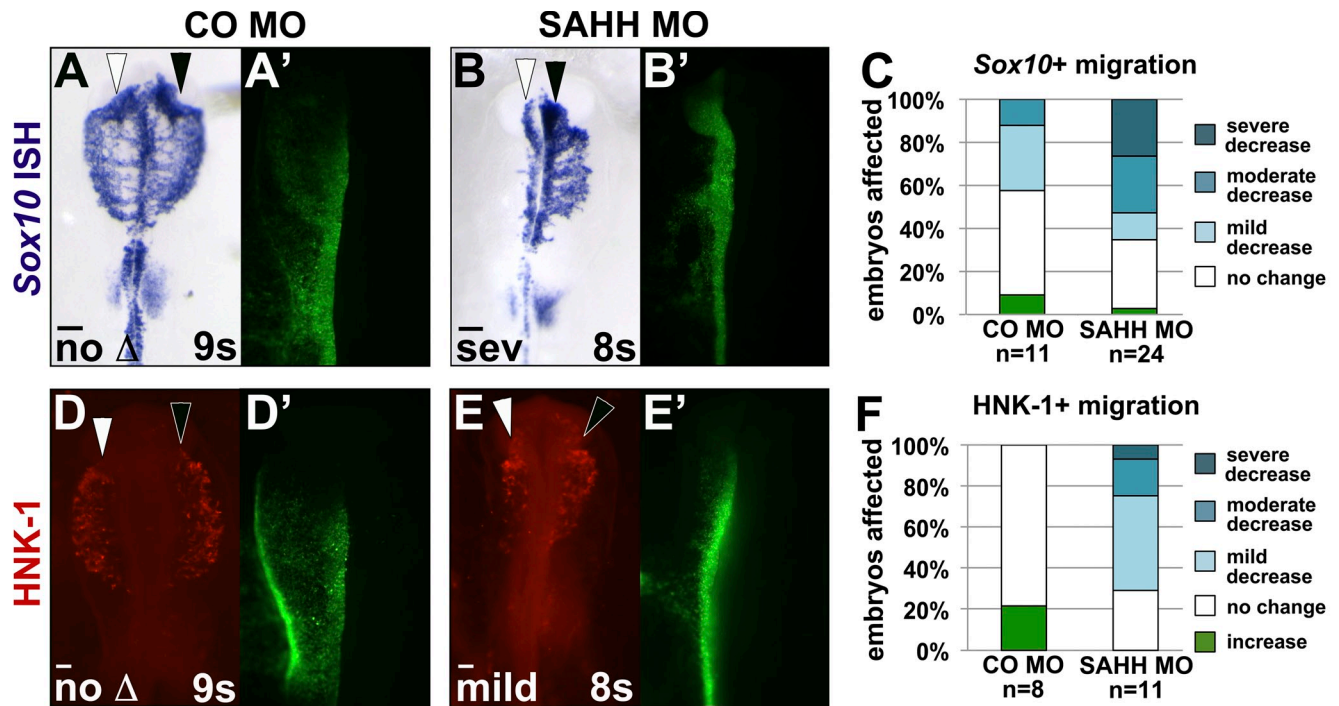
Figure 2. **SAHH is required for neural crest cell migration.** Embryos were unilaterally electroporated with standard control MO (CO MO; A' and D', green) or SAHH MO (B' and E', green) at late gastrula and reincubated to 8–10 somites (s). Migratory neural crest cells were visualized by in situ hybridization for *Sox10* (A and B, purple) or immunofluorescence for HNK-1 (D and E, red). White arrowhead, targeted side of embryo; black arrowhead, untargeted side of embryo. (A, B, D, and E) Neural crest migration distance is reduced in neural crest cells targeted with SAHH MO (*Sox10* representative example shown in B, $P = 2.05 \times 10^{-4}$; HNK-1 representative example shown in E, $P = 0.04$). (C and F) Stacked bar graphs depicting the frequency and severity of *Sox10* (C) or HNK-1 (F) visualized migration defects in embryos electroporated with CO MO or SAHH MO. (A, B, D, and E) dorsal views, fluorescent MO targeting in right panel. Bars, 100 µm.

SAHH localizes to the cytoplasm of migratory neural crest cells

In characterizing SAHH expression, we noted a striking subcellular localization of SAHH protein in neural crest cells. In most cells of the embryo, SAHH was nuclear (Fig. 4 A); however, SAHH immunoreactivity in HNK-1–positive migratory neural crest cells (Fig. 4 B'', outline) was more diffuse (Fig. 4 B'). High magnification views revealed that this was because neural crest cells (ncc) exhibit cytoplasmically localized SAHH protein (Fig. 4, D and D', white arrowheads) in addition to nuclear SAHH. In contrast, SAHH was primarily nuclear in surrounding cell types such as head mesenchyme (Fig. 4, D and D', mes, white arrow) and nonneural ectoderm (Fig. 4 E, nne, white arrow). To further assess this localization, we cultured individual migratory cranial neural crest cells. SAHH was expressed throughout HNK-1–positive neural crest cells (Fig. 4, F and F'''), but was most concentrated outside the nucleus, particularly in protrusions (Fig. 4 F'', white arrowheads). SAHH immunofluorescent and Western blot detection are SAHH protein dependent (Fig. S2, A–C), indicating the antibody is specific for SAHH. Notably, SAHH nuclear versus cytoplasmic localization is stage-dependent in *Xenopus* embryos, and there is some evidence that SAHH interacts with methyltransferases, potentially to localize SAHH to the site of methylation reactions and SAH production (Radomski et al., 1999, 2002; Lee et al., 2012). Thus, the cytoplasmic localization of SAHH led us to postulate that SAHH, and methylation, act outside of the nucleus in migratory neural crest cells.

Migratory neural crest cells contain cytoplasmic methylated proteins

If nonnuclear methylation regulates neural crest migration, methylated proteins should be present in the cytoplasm of neural crest cells. Because other work in our laboratory has identified a neural crest–essential lysine dimethylase (unpublished data), we focused on lysine methylation and obtained an antibody against mono- or di-methylated lysines (K-me1/2; Ab23366 [Abcam]). This antibody immunofluorescently detects only lysine-methylated peptides in arrays of variously modified and unmodified peptides and is a methyl lysine–specific reagent (Levy et al., 2011). In sections of nine-somite chick embryos, K-me1/2 immunoreactivity (Fig. 5, A and B, green) largely surrounded DAPI-stained nuclei (Fig. 5, A and B, blue), consistent with known lysine methylation of diverse and abundant cellular proteins including ribosomal proteins (Ong et al., 2004; Iwabata et al., 2005; Pang et al., 2010). Strikingly, cytoplasmic K-me1/2 immunoreactivity (Fig. 5, A'' and B'', white arrowheads) was particularly prominent in HNK-1–postitive cranial migratory neural crest cells (Fig. 5, A''' [black arrowheads] and B'''). To better assess the subcellular localization of lysine-methylated proteins, we evaluated individual cultured cranial migratory neural crest cells (Fig. 5 C). In addition to bright puncta and diffuse staining in the nucleus (Fig. 5 C'', black arrow), K-me1/2 immunoreactivity was pronounced in the cytoplasm of migratory cranial neural crest cells, particularly in the periphery and in protrusions (Fig. 5 C'', white arrowheads). Although nuclear lysine methylation was
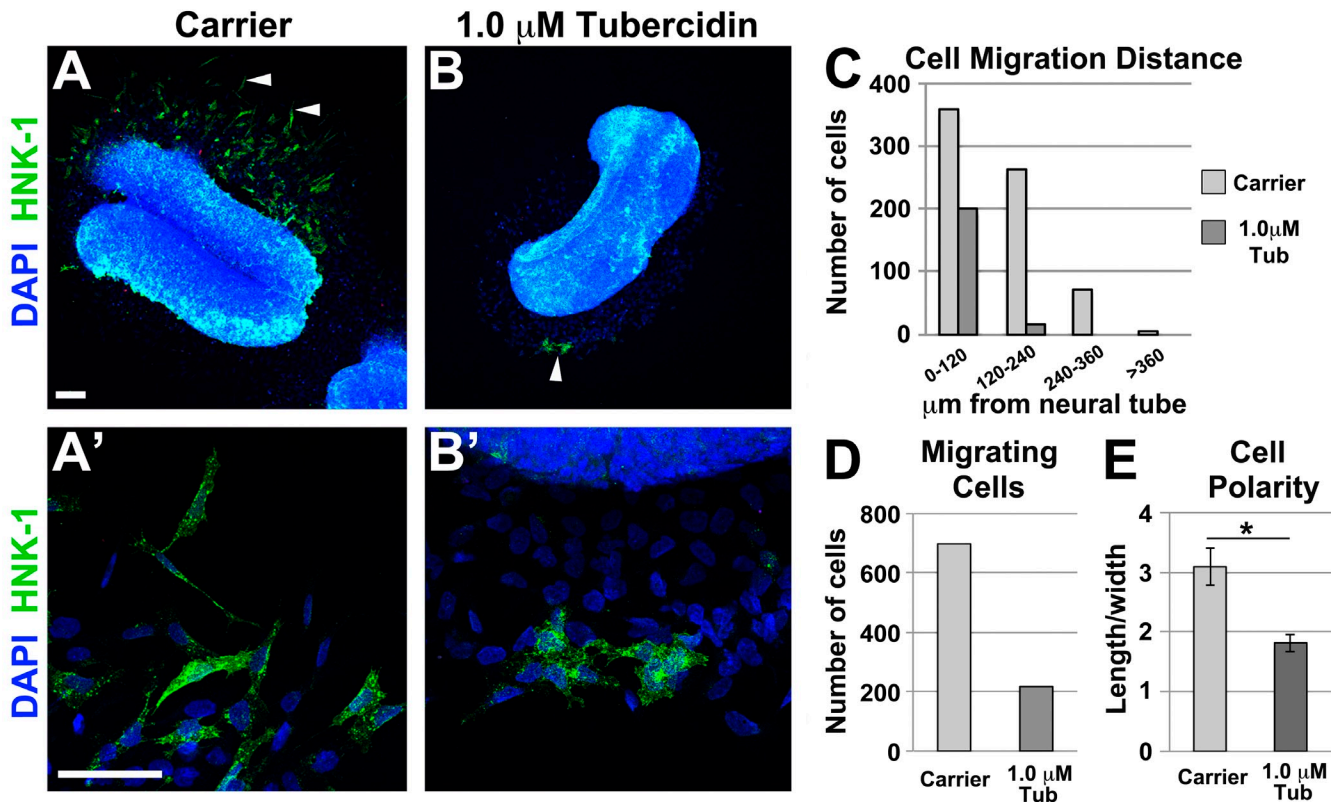
Figure 3. **Tubercidin inhibits neural crest migration and decreases neural crest cell polarity.** (A–B) Tubercidin treatment disrupts neural crest migration. Trunk neural tubes were cultured on fibronectin-coated chamber slides in carrier (A and A') or 1.0 µM tubercidin (B and B') for 24 h. Cells were stained with anti–HNK-1 (neural crest, green) and DAPI (nucleus, blue). While numerous (A, white arrowheads) polarized and elongated (A') neural crest cells migrate from carrier-treated explants, tubercidin treatment limits migration (B) and alters neural crest cell morphology (B'). Bars, 100 µm. (C) Bar graph depicting neural crest migration distance. HNK-1–positive neural crest cells from seven explants in each condition were measured and counted according to their distance away from the neural tube. In tubercidin, fewer neural crest cells emigrate, and these cells travel shorter distances. (D) Bar graph depicting the total number of HNK-1–positive neural crest cells migrating away from seven control or seven tubercidin-treated neural tubes. (E) Bar graph depicting length/width ratios, or polarity, of carrier- and tubercidin-treated neural crest cells. Tubercidin-treated neural crest cells were significantly less polarized (closer to 1, symmetrical) compared with carrier-treated neural crest cells (P = 3.3×10^{-4}).

expected given extensive histone methylation, and some cytoplasmic methyl lysine immunoreactivity was anticipated, the abundance of cytoplasmic lysine methylation in migratory neural crest cells suggested a role during neural crest migration.

Proteomic analysis of neural crest cytoplasmic-methylated proteins identified numerous cytoskeletal-associated proteins

Motivated by these results, we devised a proteomic screen to identify cytoplasmic lysine-methylated proteins in migratory neural crest cells (Fig. 6 A). We tested several strategies to isolate neural crest cells for profiling, including expansion of neural crest cells in culture (Etchevers, 2011) and antibody-based separation (Lee and Lwigale, 2008); however, in our hands, cultured neural crest cells differentiated and immune selection produced a mixed population of cells. Instead, we found that manual dissection of dorsal neural folds provided the most controlled harvest of neural crest tissue. Cranial neural folds were cultured to obtain neural crest cells at two time points during migration: emigrating (Fig. 6, "E"; 3 h in culture) and actively migrating (Fig. 6, "A"; 16–36 h in culture and remaining neural fold discarded). Approximately 400 µg of cytoplasmic protein lysate was prepared from each tissue population (E, 400 explants; A,

1,200 explants), and proteins with mono- and di-methylated lysines were immunopurified and separated by SDS-PAGE. Tryptic peptides were identified by liquid chromatography coupled to tandem mass spectrometry with electrospray ionization (LC/ESI/MS/MS). Two replicates of this method identified 182 proteins with high confidence (Table S1). This list included several known lysine-methylated proteins, such as β-actin, α-tubulin, and ribosomal proteins (Iwabata et al., 2005; Pang et al., 2010; Xiao et al., 2010), validating the outcome of the screen. Of these 182 proteins, 19 are known to participate in or regulate the cytoskeleton and were of particular interest. This category included several proteins that are important for regulating cell migration, such as actin-depolymerizing factor, myosin 9, tropomyosin α-1, and several forms of tubulin (Fig. 6 B; Vermillion et al., 2013).

Elongation factor 1-α 1: A lysine-methylated protein in migratory neural crest cells

Due to the limits of embryonic sample collection and the quantity of protein necessary for mass spectrometry (MS), as well as the known challenge of identifying methyl modifications by MS (Ong et al., 2004; Moore et al., 2013), our proteomic screening
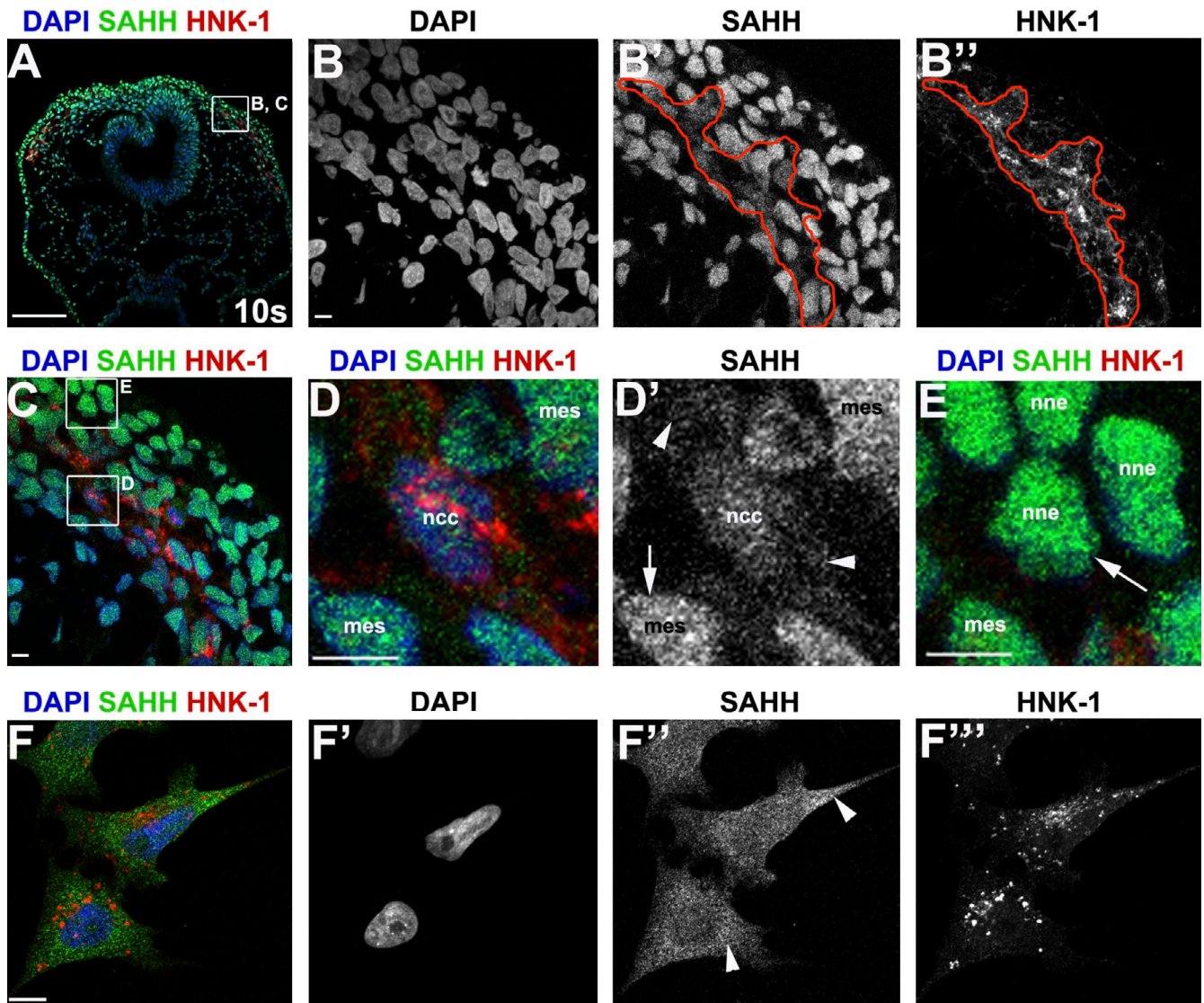
Figure 4. **SAHH is cytoplasmically localized in migratory neural crest cells.** 10 somite (s) chick embryo cross sections (A–E) and cultured cranial neural crest cells (F) immunostained for SAHH (B', D', and F'', green), HNK-1 (neural crest; B'' and F''', red), and DAPI (nuclei; B and F', blue). (A) In embryos, SAHH immunoreactivity is widespread and nuclear. (B) A higher magnification view shows that SAHH immunoreactivity (B') is more diffuse in HNK-1–positive (B'') migratory neural crest cells (red outline). (C–E) At high magnification SAHH immunoreactivity is cytoplasmic (D', white arrowheads) in neural crest cells (ncc), while SAHH is nuclear (D' and E, white arrows) in head mesenchyme (mes) and nonneural ectoderm (nne). (F) In cultured cranial migratory neural crest cells (HNK-1–positive; F'''), SAHH (F'') is abundant in the cytoplasm (white arrowheads). (A–E) Transverse sections, dorsal up. (A–F) Maximum intensity projections of confocal z-stacks. Bars: (A) 100 µm; (all others) 5 µm.

generally did not identify methylated peptides; one exception was eukaryotic elongation factor 1-α 1 (EF1α1). MS analysis showed that EF1α1 was methylated at five lysine residues in chick neural crest cells (Lys 79 and Lys 316 were tri-methylated, whereas Lys 55, Lys 165, and Lys 290 were dimethylated). Methylation of lysines 55, 165, and 316 was identified with high confidence. Four of these five methylated residues (lysine 55, 79, 165, and 316) have been previously identified in rabbit and human cells, whereas two (Lys 79 and 316) have been identified in yeast, supporting their designation as methylated lysines in chick (Dever et al., 1989; Cavallius et al., 1993; Magrane and Consortium, 2011). Lys 290 is a novel methylated residue, not previously identified as methylated in any organism. As EF1α1 methylation is not required for translation (Sherman and Sypherd, 1989; Cavallius et al., 1997), the function of EF1α1 methylation is unknown.

EF1α1 is primarily known as a component of the translation machinery that shuttles tRNA into the ribosomal A position (Slobin, 1980); however, due to the molar excess of EF1α1 compared with other translation components in the cell, it also serves as an actin-binding protein (Dharmawardhane et al., 1991; Collings et al., 1994; Edmonds et al., 1995). In particular, EF1α1 binds both actin filaments and actin mRNA at the leading edge of polarized migratory cells (Liu et al., 2002). β-Actin mRNA targeting to the leading edge is required for migratory cell polarity and movement (Kislauskis et al., 1994, 1997) and is thought to enable localized actin translation to facilitate actin polymerization for motility (Condeelis and Singer, 2005). Based on this established role of EF1α1 in motility, we examined EF1α1 localization in cultured cranial migratory neural crest cells. EF1α1 immunoreactivity is concentrated around the nucleus,
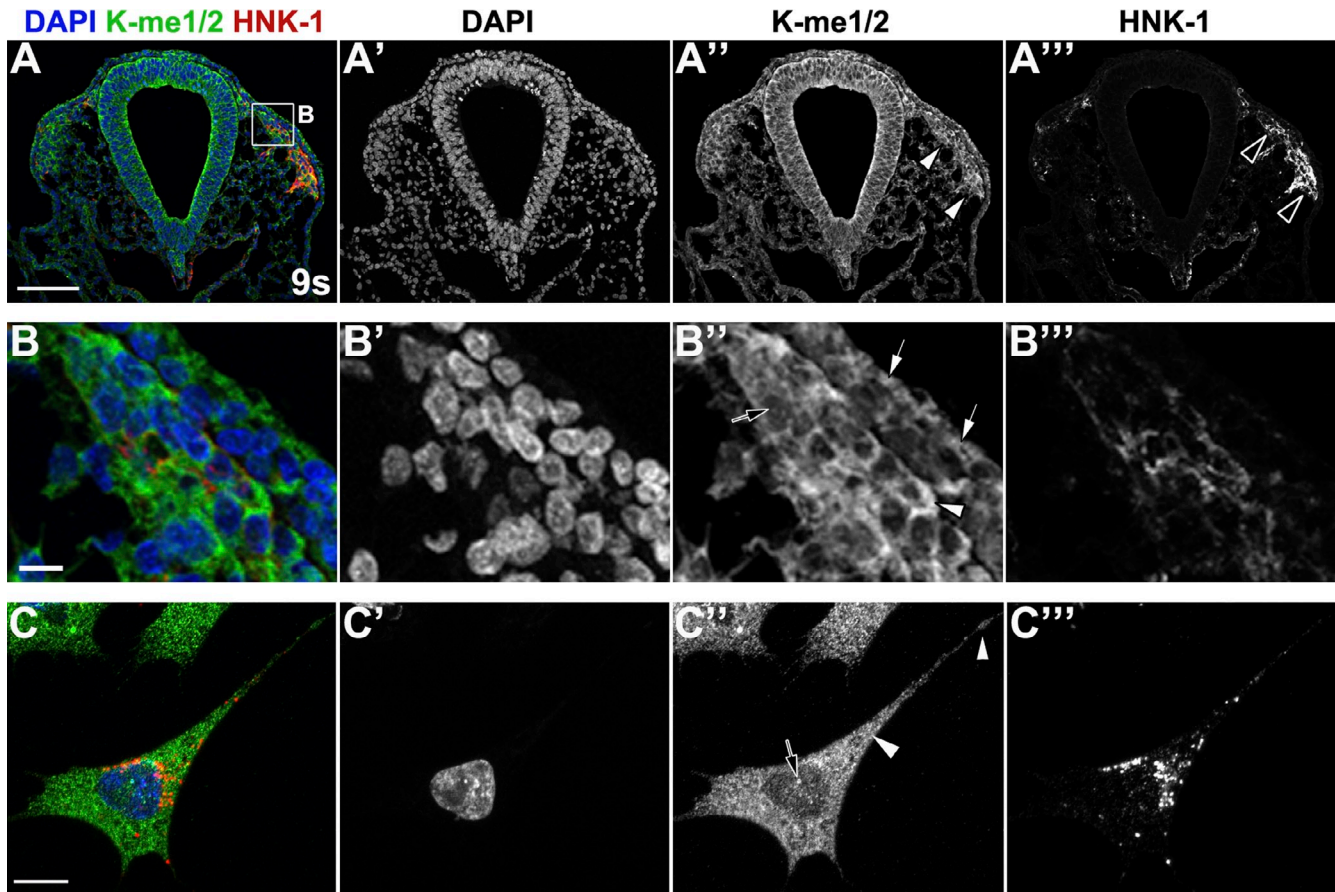
Figure 5. **Migratory neural crest cells have cytoplasmic methylated proteins.** Chick 9 somite (s) midbrain sections (A and B) or cranial neural crest cell cultures (C) immunostained for mono-/di-methylated lysine (K-me1/2; A''–C'', green), HNK-1 (neural crest; A'''–C''', red), and DAPI (nucleus; A'–C', blue). (A) Lysine-methylated proteins (A'', white arrowheads) are enriched in migratory neural crest cells (A''', black arrowheads). (B) A higher magnification view shows that lysine-methylated proteins (B'') are present in the nucleus (black arrow) and cytoplasm (white arrow) of all cell types, but enriched (white arrowhead) in the cytoplasm of HNK-1–positive migratory neural crest cells (B'''). (C) Individual cultured migratory neural crest cells (C''') have lysine-methylated proteins in the nucleus (C'', black arrow) and peripherally localized in the cytoplasm (C'', white arrowheads). (A–B) Transverse sections, dorsal up. (A–C) Maximum intensity projections of confocal z-stacks. Bars: (A) 10 μm; (B and C) 100 μm.

but is also readily apparent as filamentous staining in the periphery (Fig. 7, A–A', white arrowhead). Co-staining with phalloidin shows EF1α1 colocalization with actin filaments (Fig. 7 A'') and at higher magnification shows colocalization along actin filaments in lamella (Fig. 7, B–B'', white arrowheads) and filopodia (Fig. 7, C–C'', white arrowheads). That EF1α1 exhibits strong, filamentous, peripheral localization and is methylated on several lysines in neural crest cells, along with the established role of EF1α1 in motility, made EF1α1 an excellent candidate cytoplasmic protein to be regulated by methylation during neural crest migration.

EF1α1 methylation is required for neural crest migration

To determine whether EF1α1 methylation is functionally relevant for neural crest migration, we created methylation-resistant EF1α1 by mutating to alanine the six lysines that are methylated in chick and/or human (EF1α1-6x-methyl mutant, or EF1α1-6xMM). We reasoned that, when overexpressed, EF1α1-6xMM would compete with endogenous EF1α1 to incorporate into complexes and bind actin. If EF1α1 methylation is required for

an event in neural crest development, the inclusion of methylation-resistant EF1α1 should disrupt that event, even in a background of wild-type EF1α1. Knocking down and replacing EF1α1 with the 6x-methyl mutant was another option; however, we did not pursue this approach because EF1α1 is an essential component of the basal translation machinery (Riis et al., 1990). Moreover, EF1α1 can either prevent or promote actin polymerization depending on its cellular concentration (Murray et al., 1996) and EF1α1 levels are developmentally regulated (Gao et al., 1997), thus exact replacement by overexpression would be difficult.

First, we evaluated whether EF1α1 was correctly localized when fused to GFP and driven from a chick expression construct in cultured neural crest cells. EF1α1-GFP and EF1α1-6xMM-GFP localization resembled the pattern of endogenous EF1α1 immunofluorescence (Fig. 7): GFP fusion proteins were abundant around the nucleus and formed strands within the cell body and in protrusions (Fig. S5, A–F). Thus, EF1α1-GFP and EF1α1-6xMM-GFP were found in the same locations as endogenous EF1α1, suggesting GFP fusion and lysine mutations do not prevent EF1α1 from incorporating into migration-related structures.

A

Cranial neural folds

Culture 3 hours

E = emigrating

Culture 16 hours

A = actively migrating

Cytoplasmic lysate

Mono/di-methyl-lysine IP

CH₃

CH₃

relative abundance

m/z

LC/ESI/MS/MS

B

Cytoskeletal-related proteins

Actin, alpha skeletal muscle
Actin, cytoplasmic
Actin-depolymerizing factor
Beta-actin
c-beta-3-beta-tubulin
Elongation factor 1-alpha 1
Fibroblast alpha-actinin
Filamin
Myosin-9
Myosin-10
Myosin-11
Myosin light polypeptide 6
Myosin regulatory light chain 2,
  isoform L20-B21
Spectrin, alpha chain, brain
Tropomyosin alpha-1 chain
Tubulin-alpha-1 chain
Tubulin beta-2 chain
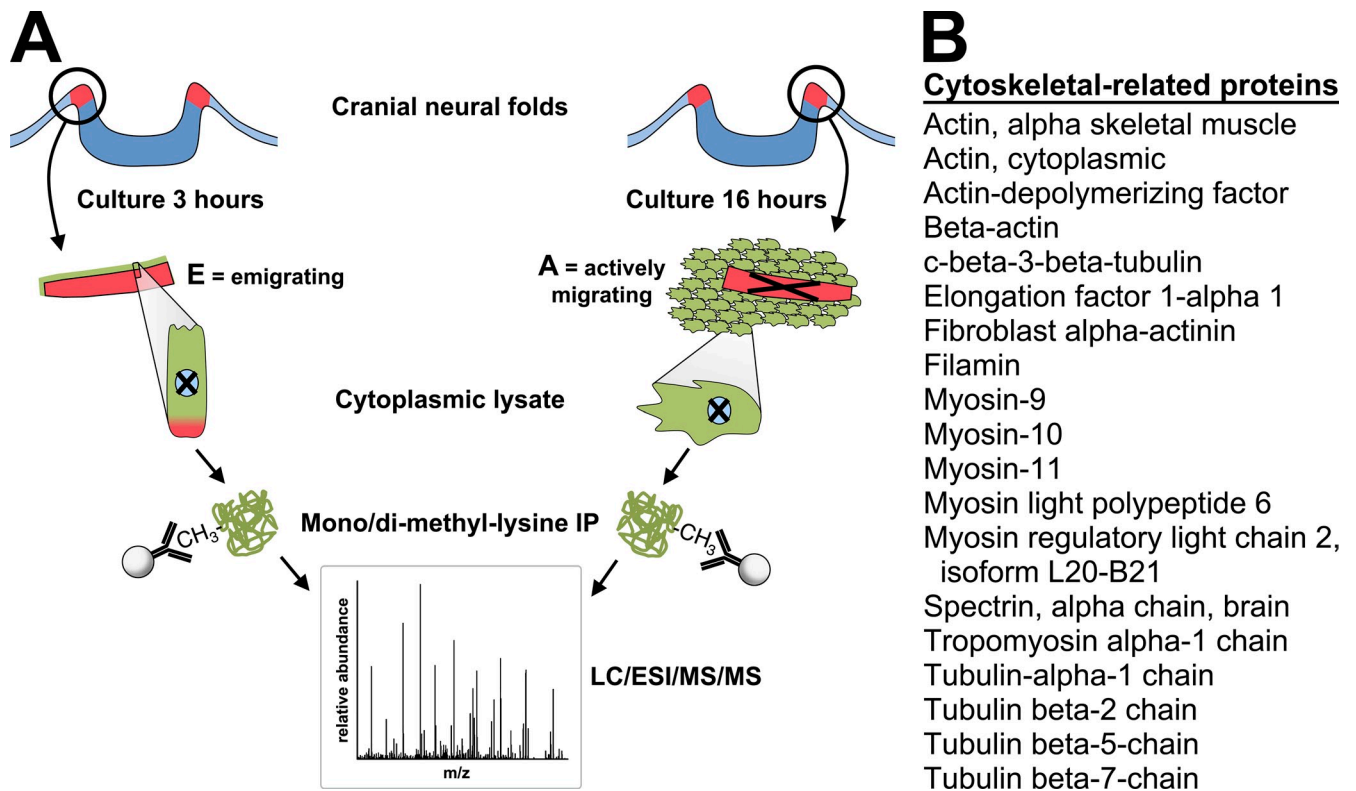Tubulin beta-5-chain
Tubulin beta-7-chain

Figure 6. **Proteomic profiling of lysine-methylated proteins identifies several cytoskeletal-related proteins.** (A) Cytoplasmic methylated proteins were identified at two different time points during neural crest migration. Cranial neural folds were cultured for 3 h to obtain emigrating (E) neural crest cells, or 16–36 h with removal of the remaining neural fold to collect actively migrating (A) neural crest cells. Cytoplasmic fractions were prepared and immuno-precipitated using the antibody against mono- and di-methylated lysines. Immunoprecipitated proteins were separated by SDS-PAGE and were silver or Coomassie stained. Tryptic peptides were identified by liquid chromatography coupled to tandem mass spectrometry with electrospray ionization (LC/ESI/MS/MS). (B) Putatively methylated cytoplasmic proteins identified with high confidence that are involved in the cytoskeleton.

Next, we overexpressed EF1α1-6xMM to disrupt EF1α1 methylation in neural crest cells. Vector only, EF1α1-GFP and EF1α1-6xMM-GFP were unilaterally targeted into chick neural crest precursors at late gastrula. Embryos were incubated 8–12 h to 4–6 somites to evaluate specification, or 14–20 h to 8–10 somites to assay effects on migration. In either case, neural crest cells were visualized by *Sox10* in situ hybridization. In contrast to vector-only electroporation (pMES; Fig. 8, A, D, E, and H), overexpressing wild-type EF1α1 had variable effects on neural crest development. In specified neural crest cells, *Sox10* expression ranged from increased to severely decreased, with the majority of embryos showing no phenotype compared with the untargeted side (Fig. 8, B [white arrowhead] and D; P = 0.02). Neural crest migration distance was also variable, with the majority of wild-type EF1α1-targeted neural crest cells exhibiting mild migration defects when comparing the targeted to untargeted side of the embryo (Fig. 8, F [white arrowhead] and H; P = 0.09). Thus, cells are sensitive to EF1α1 dose, consistent with the observation that EF1α1 can either promote or inhibit actin polymerization at different concentrations (Murray et al., 1996). At 4–6 somites, EF1α1-6xMM elicited a similar range of neural crest specification phenotypes as wild-type EF1α1 (Fig. 8, C [white arrowhead] and D; P = 0.02 compared with pMES, P = 0.72 compared with EF1α1). This suggests the K to A mutations did not disrupt EF1α1 activity during specification, much as a methylation-resistant EF1α does not affect translation in yeast

(Cavallius et al., 1997). In contrast, at 8–10 somites, electroporation of the EF1α1-6xMM blocked neural crest migration in most embryos (Fig. 8, G [white arrowhead] and H; P = 4.66×10^{-7} compared with pMES, P = 6.82×10^{-4} compared with EF1α1). This migration defect was not due to cell death (Fig. S5, H and I). Moreover, EF1α1-6xMM did not disrupt down-regulation of the cranial neural crest epithelial cadherin6B, indicating that this feature of epithelial-to-mesenchymal transition preceding migration took place on schedule (Fig. S5 J). Together, these data reveal that EF1α1-methylated lysines are essential for neural crest migration and demonstrate a novel role for nonhistone protein methylation during neural crest migration.

Discussion

Although data in the literature are consistent with a role for nonhistone protein methylation in eukaryotic cell migration, direct evidence, particularly during development, is lacking. This study defines the importance of nonhistone protein methylation during neural crest migration. We show that the methylation cycle enzyme SAHH is required for neural crest cells to migrate away from the neural tube, revealing for the first time that methylation is essential for neural crest migration. Cytoplasmic localization of SAHH and lysine-methylated proteins in migratory neural crest cells motivated a proteomic screen, which identified an extensive list of methylated and putatively methylated
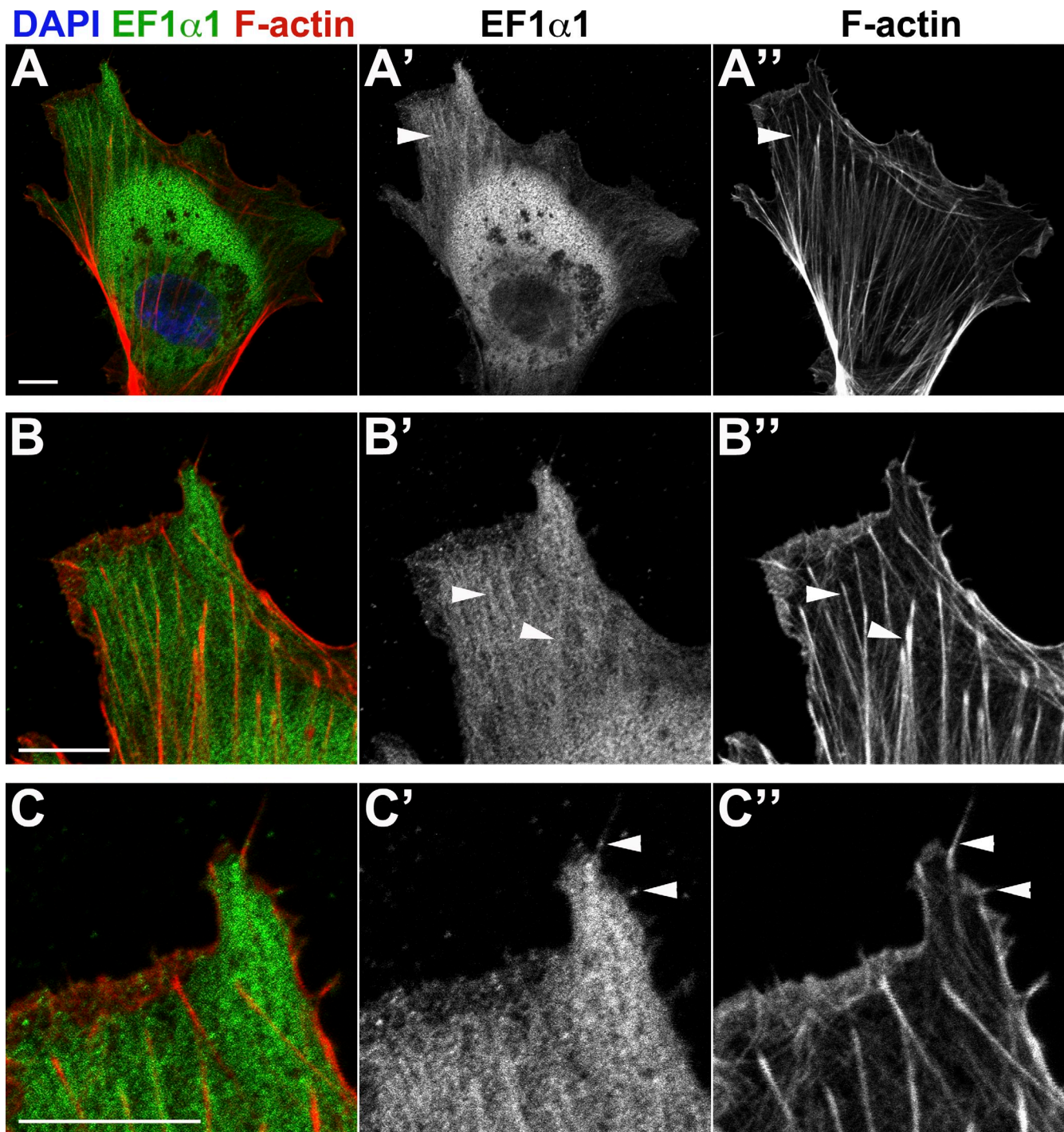
Figure 7. EF1α1 colocalizes with F-actin in the cytoplasm of migratory neural crest cells. Cranial neural crest cultures immunostained for elongation factor 1-α 1 (EF1α1; A'–C', green), F-actin (phalloidin; A''–C'', red), and DAPI (nucleus; blue). (A) EF1α1 (A', white arrowhead) is expressed in migratory neural crest cells and colocalizes with F-actin filaments (A'', white arrowhead). (B–C) Higher magnification views show colocalization of EF1α1 with F-actin in lamella (B' and B'', white arrowheads) and filopodia (C' and C'', white arrowheads). Bars, 10 μm.

nonhistone proteins. Characterization of one of these proteins, the actin-binding protein EF1α1, showed that its methylated lysines are required for neural crest migration. Taken together, our data show that nonhistone protein methylation, in particular methylation of EF1α1, is essential for neural crest migration.

Although the focus of our analysis was migration, our experiments also give insight into neural crest specification. In SAHH MO–electroporated embryos assayed at four somites,

we noted a striking difference: *Snail2* expression was minimally disrupted (Fig.1, A–C), while *Sox10* expression was moderately or severely reduced in half the embryos analyzed (Fig. 1, D–F). First of all, this indicates that methylation became inhibited in SAHH MO–electroporated embryos during specification. Neural crest specification requires DNA methyltransferase 3A (DNMT3A) to silence neural transcription factors *Sox2* and *Sox3* that repress *Snail2* and *Sox10* expression (Hu et al., 2012). Because *Snail2*
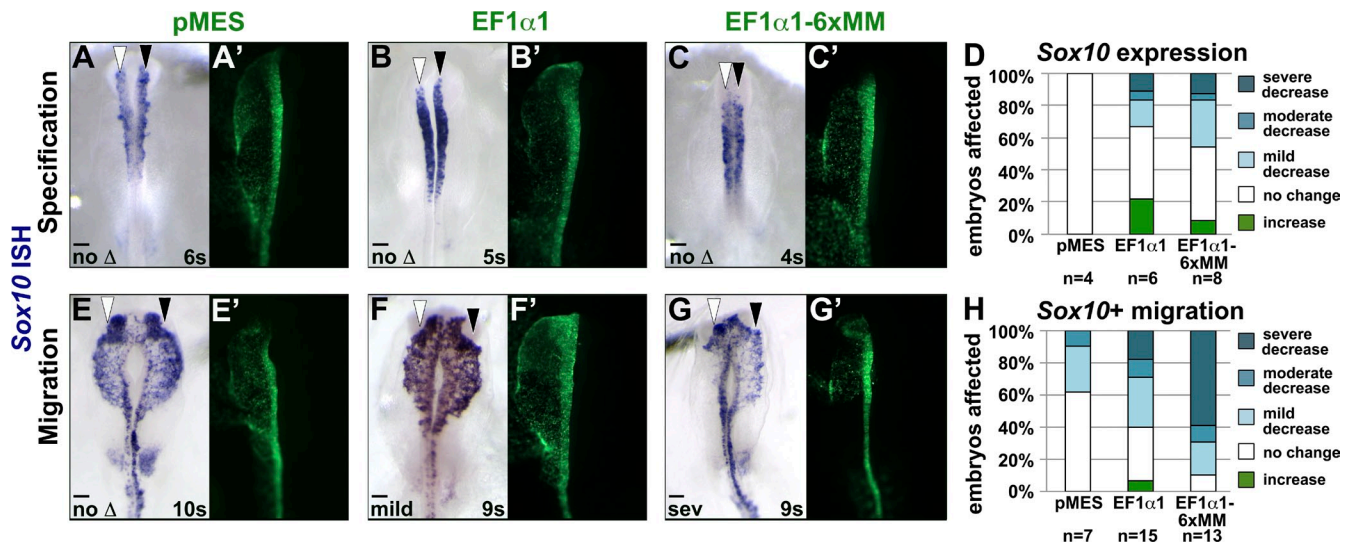
Figure 8. **EF1α1 methylation is required for neural crest migration.** Embryos were unilaterally electroporated with pMES vector DNA (pMES; A' and E', green), pMES-EF1α1-GFP fusion (EF1α1; B' and F', green), or pMES-EF1α1-6x-methyl mutant (EF1α1-6xMM; C' and G', green) at late gastrula. At 4–6 somites (A–C) or 8–10 somites (E–G), embryos were collected and *Sox10* expression was assessed by in situ hybridization (purple). White arrowhead, targeted side of embryo; black arrowhead, untargeted side of embryo. (A–C) EF1α1-6xMM effects on specification resemble EF1α1. *Sox10* expression is unchanged on the targeted side by pMES, EF1α1, or EF1α1-6xMM electroporation in the majority of embryos. (D) Stacked bar graph depicting the frequency and severity of *Sox10* expression defects in embryos overexpressing pMES, EF1α1, or EF1α1-6xMM. (E–G) EF1α1-6xMM blocks neural crest migration. pMES electroporation does not affect neural crest migration distance on the targeted side (E), while EF1α1 electroporation elicits a broad range of phenotypes, with most embryos being mildly affected (F). EF1α1-6xMM electroporation severely decreased neural crest cell migration distance on the targeted compared with the untargeted side of the embryo (G). (H) Stacked bar graph depicting the frequency and severity of migration defects in embryos electroporated with pMES, EF1α1, or EF1α1-6xMM, showing that overexpression of EF1α1-6xMM significantly decreases neural crest migration compared with pMES or EF1α1 (P = 4.66 × 10^{-7}; P = 6.81 × 10^{-4}, respectively). (A–C and E–G) Dorsal views of in situ hybridization on left, fluorescent MO targeting on right. Bars, 100 μm.

was expressed (Fig. 1 B), SAHH protein turnover (Fig. S2) and the resulting accumulation of SAH must inhibit methyltransferases after the critical period for DNMT3A activity. Second, the distinct effects of SAHH knockdown on *Snail2* and *Sox10* expression support their placement in the neural crest transcriptional hierarchy: *Snail2* is regulated by neural plate border specifiers, while *Sox10* is turned on later in response to other neural crest transcription factors (Prasad et al., 2012). SAHH knockdown-dependent inhibition of methyltransferase activity likely occurs after *Snail2* up-regulation, but before activation of *Sox10* expression. Third, our results are consistent with differential epigenetic regulation of *Sox10* and *Snail2*, as the lysine methyltransferase NSD3 is required for histone H3 lysine 36 methylation of *Sox10* but not *Snail2* (unpublished data). The idea that these genes are regulated by different methyltransferases or marked with different combinations of methyl marks that decay at different rates in a state of methyltransferase inhibition (Barth and Imhof, 2010) is consistent with our data. Further characterization of NSD3, identification of other neural crest methyltransferases, and analysis of methylation is needed to evaluate these possible mechanisms.

The neural crest methyl proteome offers an unprecedented view of cytoplasmic protein methylation in a migratory cell type. Given the importance of post-translational modifications like phosphorylation in migration (Rottner and Stradal, 2011; Y. Zhang et al., 2012), we were intrigued by the abundance of lysine-methylated proteins in the cytoplasm of migratory neural crest cells (Fig. 5 C′′, white arrow) and set out to profile these proteins. Our efforts identified 182 methylated and putatively methylated

proteins, providing the first view of this level of regulation during cell migration. Although extensive, this collection is likely not exhaustive; for most proteins only a few peptides were identified, and these peptides generally did not contain the methylated residue. Peptide coverage for each protein and the number of proteins identified were undoubtedly limited by the amount of embryonic sample we were able to obtain. As a result, failure to identify a peptide in the spectra does not necessarily mean it is absent from the tissue, and comparison between time points is not possible. Moreover, it is a known challenge to identify methyl modifications by mass spectrometry, due to the size of the resulting mass shift and three possible states (mono, di, tri), as well as the fact that lysine methylation can prevent trypsin digestion and affect subsequent detection (Ong et al., 2004). Even in yeast, where sample collection is nonlimiting and metabolic labeling strategies can be applied, profiling has identified limited methylated peptides (Moore et al., 2013). Despite these challenges, we identified five methylated lysines in EF1α1, four of which are validated by work in other systems (Dever et al., 1989; Cavallius et al., 1993; Magrane and Consortium, 2011), lending support to our analysis.

In addition to the identification of EF1α1-methylated lysines, several features indicate that this is a high quality profile. First, all proteins were identified with high confidence. Moreover, we identified many known lysine-methylated proteins. Ribosomal proteins formed the largest category (Table S1), and ribosomal proteins, including the 60S ribosomal protein L27 and the 40S ribosomal protein S13 we identified, are lysine methylated (Pang et al., 2010; Levy et al., 2011). β-Actin, α-tubulin,

and EF1α1 are also known lysine-methylated proteins (Cavallius et al., 1993; Iwabata et al., 2005; Xiao et al., 2010). Finally, although we prepared cytoplasmic extracts with an established, commercially available reagent, cross-contamination with nuclear proteins is expected to be ∼10% (Thermo Fisher Scientific). Thus, we identified histone proteins, including all four core histones that are well characterized for their lysine methylation (Young et al., 2010) and further support our profile. Putting this all together, it is likely we were able to detect EF1α1 because it is methylated at multiple lysines and due to its sheer abundance within cells. This is consistent with and undoubtedly accounts for much of the elevated cytoplasmic K-me1/2 immunoreactivity in migratory neural crest cells (Fig. 5). In sum, this collection of putatively methylated, nonhistone proteins provides an exciting first glimpse of cytoplasmic nonhistone protein methylation during neural crest migration and is an important resource for future studies to determine the function, extent, and stability of methyl marks on nonhistone proteins.

As a functional validation of the screen and our hypothesis that nonhistone protein methylation regulates neural crest migration, we showed that neural crest cells expressing methylation-resistant EF1α1 fail to migrate (Fig. 8). Although EF1α1 methylation was first detected three decades ago, and EF1α1-specific methyltransferases have been identified in yeast, the function of EF1α1 methylation is unclear (Hiatt et al., 1982; Lipson et al., 2010; Couttas et al., 2012). All evidence suggests that it is not required for translation (Sherman and Sypherd, 1989; Cavallius et al., 1997; Polevoda and Sherman, 2007). Given this, and the fact that EF1α1 regulates the actin cytoskeleton in migrating cells, it was intriguing to identify it as a cytoplasmic methylated protein in migratory neural crest cells (Fig. 6). Indeed, in comparison to EF1α1 overexpression, which consistently elicited a wide range of effects on specification and migration, a methylation-resistant form of EF1α1 specifically blocked neural crest migration (Fig. 8). This phenotype is particularly striking because methylated and unmethylated EF1α1 are equivalent in translation assays (Sherman and Sypherd, 1989), and yeast with methylation-resistant EF1α1 are phenotypically normal (Cavallius et al., 1997). Methyl mutant EF1α1 did not disrupt down-regulation of the cranial epithelial cadherin, cadherin6B (Fig. S5 J), and some neural crest cells emerged from EF1α1-6xMM-GFP–electroporated neural folds (Fig. S5, D–F), implying that epithelial-to-mesenchymal transition can take place when EF1α1 methylation is defective. This suggests that EF1α1 methylation is required for motility, potentially to regulate EF1α1's role in the actin cytoskeleton (Condeelis and Singer, 2005). In combination with SAHH MO knockdown (Fig. 2) and tubercidin experiments (Fig. 3), these data also reveal that cytoplasmic protein methylation is essential for neural crest migration.

What is the function of EF1α1 methylation during migration? Methylation-resistant EF1α1 was not mislocalized and still found in strand formations (Fig. S5, D–F); thus, EF1α1 methylation is unlikely to affect binding to actin filaments. One possibility is that methylation-resistant EF1α1 disrupts EF1α1 protein–protein interactions that are required for local actin translation, nucleating actin polymerization, or other actin-related functions. Indeed, there is evidence to suggest that EF1α1 methylation

alters its protein–protein interactions (Sherman and Sypherd, 1989). EF1α1 methylation could also be required for β-actin mRNA binding and targeting (Condeelis and Singer, 2005). In favor of this, β-actin mRNA targeting to the leading edge is required for cell polarization and motility (Kislauskis et al., 1994, 1997), as is methylation (Figs. 2 and 3), although disrupting EF1α1 methylation does not lead to a statistically significant reduction in neural crest cell polarity (Fig. S5 G). EF1α1 was lysine methylated at both E and A migration time points, suggesting it is involved throughout neural crest migration. Whatever the role of EF1α1 methylation, it is a migration-specific function, as neural crest specification was equivalently affected by overexpression of wild-type EF1α1 or EF1α1-6xMM (Fig. 8), consistent with previous reports that EF1α1 methylation is dispensable for translation-related activities (Sherman and Sypherd, 1989; Cavallius et al., 1997). These findings expand our view to include nonhistone methylation as a novel layer of posttranslational control in the neural crest, and open new avenues of research to understand the mechanism by which EF1α1 methylation regulates cell migration.

Materials and methods

Embryos
Fertilized chicken embryos were obtained from local sources. Eggs were incubated at 37°C in a humidified incubator until the desired stage of development (Hamburger and Hamilton, 1992), judged by counting somite pairs.

Morpholinos and DNA constructs
FITC-tagged morpholinos (MOs) were synthesized by GeneTools, LLC with the following sequences: translation blocking SAHH MO 5′-CAGCCTGTC-CGACATGCTGGAGGCA-3′; and standard control MO 5′-CCTCTTACCT-CAGTTACAATTTATA-3′ (CO MO). For SAHH overexpression and rescue, full-length SAHH was subcloned into pMES-mCherry (Roffers-Agarwal et al., 2012). Full-length chick EF1α1 was PCR amplified to include terminal EcoRI and SspI sites. The internal ribosome entry site in pMES (Swartz et al., 2001) was excised by EcoRI–MscI digest, and chick EF1α1 was inserted to create an in-frame EF1α1-GFP fusion. Methylation site mutations were made using the QuikChange Multi Site-Directed Mutagenesis kit (Agilent Technologies).

Electroporation
Ex ovo early embryo electroporation was performed on late gastrula stage 4–5 embryos as described previously (Gammill and Krull, 2011; Roffers-Agarwal et al., 2012). In brief, embryos were adhered to Whatman filter paper, isolated from the yolk, rinsed in chick Ringer's saline, and placed in fresh Ringer's in an electroporation cuvette with a 4-mm gap. 1.0 mM MO (SAHH or control) or 3 µg/µl DNA (EF1α1 constructs or pMES vector) was injected from the ventral side into the subvitelline space adjacent to neural crest precursors and electroporated using five square-wave 7 V 50-msec pulses with 100-msec gaps. Embryos were then cultured on agar-albumin plates until the desired stage.

Neural crest cultures
Cranial neural folds were dissected from 4–7 somite embryos. Stage 16 trunk neural tubes were prepared by explanting the region of the last 10 formed somite pairs, incubating the tissue in dispase solution (1.2 U/ml; Life Technologies) on ice for 15 min followed by 10 min at 37°C, and aspirating through a fire-polished Pasteur pipette to separate the neural tube from surrounding tissues. Cranial or trunk explants were then cultured for 16–24 h at 37°C on 10–100 µg/ml fibronectin-coated glass coverslips (Thermo Fisher Scientific) in neural crest complete media (L15, 1% L-glutamine, 0.1% penicillin/streptomycin [all from Life Technologies], 10% FBS [VWR Scientific], and 10% chick embryo extract [Bronner-Fraser and García-Castro, 2008]). For evaluation, cultures were fixed in 4% paraformaldehyde and permeabilized in PBS + 1.0% Triton X-100.

Tubercidin
A 150-mM stock of tubercidin (Sigma-Aldrich) was prepared in 8.7 M (50%) acetic acid. Trunk neural tubes were incubated in chamber slides (Thermo Fisher Scientific) with neural crest complete media containing 58 µM acetic acid (carrier) or 0.1–1.0 µM tubercidin (58 µM final concentration of acetic acid). Well dividers were removed and slides were fixed and immunostained as indicated.

In situ hybridization
SAHH (Adams et al., 2008), *Snail2* (Gammill and Bronner-Fraser, 2002), and *Sox10* (Cheng et al., 2000) digoxigenin-labeled probes were synthesized and chick embryos processed by whole-mount chick in situ hybridization, as described previously (Wilkinson, 1992).

Histology
Embryos were infiltrated with 5% and 15% sucrose, embedded in gelatin in 15% sucrose, frozen in liquid nitrogen, and sectioned with a cryostat (model CM1900; Leica) at 10–20 µm. Gelatin was removed from the sections by incubating for 30 min in 42°C PBS.

Immunostaining
Sections, cultures, and whole embryos were blocked in PBS + 10% fetal bovine serum + 0.1% Triton X-100 for 30 min at room temperature and stained with anti-HNK-1 (ATCC; Manassas, VA), anti-SAHH (anti-32-5B6; DSHB, Iowa City, IA), anti-K-me1/2 (Ab23366; Abcam), anti-EF1α1 (Abgent), anti-cleaved caspase3 (rabbit anti-cl.casp3; Cell Signaling Technology), and anti–phospho-histone H3 (rabbit anti-pH3; EMD Millipore) followed by the appropriate secondary antibody (mouse AF488, rabbit AF568, mouse AF568 [Life Technologies]; or Cy2 anti–mouse/rabbit IgG, Cy5 anti–mouse/rabbit IgG, RRX anti–mouse IgM [Jackson ImmunoResearch Laboratories, Inc.]) as indicated. For some assays the signal was amplified using a mouse anti–rabbit IgG (Jackson ImmunoResearch Laboratories, Inc.).

Microscopes and image acquisition
To visualize electroporation targeting or in situ hybridization results, whole-mount embryos were imaged in PBS + 0.1% Tween using a stereoscope (Discovery V8; Carl Zeiss) with an Achromat S 1.0× lens and fluorescence module outfitted with a GFP 500 filter cube. Images were acquired with a digital camera (AxioCam MRc5; Carl Zeiss) using Axiovision 4.8.2 software (Carl Zeiss). Slides and cultures were mounted with Permafluor (Thermo Fisher Scientific) containing 1 mg/ml DAPI. In situ hybridized sections were imaged on a microscope (Axioimager A1; Carl Zeiss) with a Plan Apochromat 20×/0.8 NA lens and acquired with the AxioCam MRc5 camera using Axiovision 4.8.2 software. Immunofluorescently labeled cells and sections were imaged using a confocal system (LSM 710; Carl Zeiss) attached to an inverted microscope (Observer Z.1; Carl Zeiss) outfitted with Plan Apochromat 10×/0.45 NA, 20×/0.8 NA, 40×/0.95 NA, and 100×/1.46 NA lenses and FS38, FS43, and FS49 filter sets. Confocal images were acquired using ZEN 2010 software (Carl Zeiss), and two-dimensional maximum intensity projections were produced from three-dimensional z-stack images using the data from the highest intensity pixels along the projection axis. All imaging was performed at room temperature. Image files were assembled in Photoshop (Adobe).

Quantification of migratory neural crest cell numbers, migration distance, and polarity
Seven neural tube explants in each condition (carrier or 1.0 µM tubercidin) were immunostained with anti–HNK-1 antibody. HNK-1–positive cells surrounding the neural tubes were counted and their distance migrated designated by their position relative to concentric boundaries drawn 120 µm, 240 µm, or 360 µm away from the borders of the neural tube. To evaluate polarity, 29 carrier-treated cells and 21 cells treated with 1.0 mM tubercidin were measured at their longest length and perpendicular width using ImageJ (National Institutes of Health; Schneider et al., 2012). Ratios of length to width were calculated in Excel (Microsoft).

Phenotype evaluation
Because electroporated constructs are inherited mosaically, phenotype was scored at the cranial axial level with maximal fluorescent MO or GFP signal in the dorsal neural tube. Effects on premigratory gene expression were analyzed in whole mount by judging the relative amount of colorimetric in situ hybridization signal on the targeted and untargeted side of the embryo (Fig. S3, A–D). A reduction encompassed both lower levels of mRNA and/or fewer specified neural crest cells. Effects on migration were evaluated by comparing the distance migrated on targeted and untargeted sides (Fig. S3, E–H). All phenotypes were scored blind by three independent judges and statistics were performed using two-sided Fisher's exact test in R (R Development Core Team, 2011).

Cell death and proliferation
For the tubercidin assay, cultures were fixed in 4% paraformaldehyde for 15 min and cell death was detected using the In-Situ Cell Death Detection kit (Roche) according to the manufacturer's instructions. For SAHH MO and EF1α1 overexpression assays, embryos were sectioned and immunostained with anti-cleaved caspase3 to assay cell death and anti–phospho-histone H3 to assay proliferation. Immunoreactive cells were counted in the dorsal half of the cranial neural tube on both the targeted and untargeted sides of the embryo for at least five sections per embryo (n = 5) and significance was evaluated by *t* test in Excel (Microsoft).

Immunoprecipitation
Emigrating neural crest cells (E) were collected from 4–7 somite cranial neural folds after they were cultured in neural crest complete media for 3 h and harvested. Actively migrating (A) neural crest cells were prepared by culturing cranial neural folds for 16–36 h, removing the neural fold, and collecting the migratory neural crest cells by 3-min treatment with trypsin-EDTA (Life Technologies). Cytoplasmic protein extracts were prepared using the NE-PER Nuclear and Cytoplasmic Extraction kit, and protein concentration was determined by BCA Assay (both from Thermo Fisher Scientific). Cytoplasmic lysates were split equally into four tubes and incubated for 30 min at room temperature with rotation in control goat IgG antibody (5 µg; R&D Systems) to preclear, and rabbit polyclonal to mono-and di-methylated lysine (K-me1/2, 5 µg; Abcam) mixed with Protein G magnetic beads (Life Technologies) to immunoprecipitate. After incubation, beads were washed three times with PBS. Proteins were eluted from the beads by boiling in water. Eluates were combined and concentrated by speed vacuum. After addition of SDS-PAGE sample buffer containing Bromophenol blue and 5% β-mercaptoethanol, protein samples were boiled. Immuno-precipitated proteins were resolved using a Mini-PROTEAN TGX 4–15% gel (Bio-Rad Laboratories) and then silver stained (SilverQuest; Life Technologies) or stained with Imperial Protein stain (Thermo Fisher Scientific) in accordance with the manufacturers' instructions. Lanes were cut into five sections, and destained according to the manufacturers' instructions.

Mass spectrometry
Excised gel pieces were trypsin digested (Shevchenko et al., 1996) using an Investigator ProPrep (Genomic Solutions) and lyophilized. For the first screen, digested peptide mixtures were desalted using C18 columns and mass spectrometry was performed on an LTQ mass spectrometer (Thermo Fisher Scientific) as described previously (Beckmann et al., 2013). Sequest (Thermo Finnigan) was set up to search the NCBI nonredundant *Gallus gallus* (September 03, 2010 version) database. Search parameters were: cysteine iodoacetamide; trypsin; instrument LTQ; and variable modifications-oxidized methionine. For the second screen, digested peptide mixtures were desalted with C18 resin according to the "Stage Tip" procedure (Rappsilber et al., 2003). Using a mass spectrometry–based approach (Lin-Moshier et al., 2013), peptides were analyzed using a mass spectrometer (Velos Orbitrap; Thermo Fisher Scientific). ProteinPilot 4.5 (Ab Sciex) searches were performed against the NCBI nonredundant *Gallus gallus* database (September 03, 2010 version) to which a contaminant database (www.thegpm.org/crap/index.html) was appended. Search parameters were: cysteine iodoacetamide; trypsin; instrument Orbi MS (1–3 ppm) Orbi MS/MS; biological modifications ID focus; special modifications-purified histones, thorough search effort; and False Discovery Rate analysis (with reversed database). Proteins included in Table S1 had two or more peptides identified with 95% confidence.

Online supplemental material
Fig. S1 shows the mRNA expression pattern of the methylation cycle enzyme SAHH. Fig. S2 shows efficacy and specificity controls for SAHH knockdown and inhibition. Fig. S3 shows neural crest phenotype categories. Fig. S4 shows SAHH MO rescue. Fig. S5 shows EF1α1 overexpression controls. Table S1 lists proteins identified by proteomic analysis. Online supplemental material is available at http://www.jcb.org/cgi/content/full/jcb.201306071/DC1.

References

Adams, M.S., L.S. Gammill, and M. Bronner-Fraser. 2008. Discovery of transcription factors and other candidate regulators of neural crest development. *Dev. Dyn.* 237:1021–1033. http://dx.doi.org/10.1002/dvdy.21513

Ammer, A.G., and S.A. Weed. 2008. Cortactin branches out: roles in regulating protrusive actin dynamics. *Cell Motil. Cytoskeleton.* 65:687–707. http://dx.doi.org/10.1002/cm.20296

Bajpai, R., D.A. Chen, A. Rada-Iglesias, J. Zhang, Y. Xiong, J. Helms, C.P. Chang, Y. Zhao, T. Swigut, and J. Wysocka. 2010. CHD7 cooperates with PBAF to control multipotent neural crest formation. *Nature.* 463:958–962. http://dx.doi.org/10.1038/nature08733

Barth, T.K., and A. Imhof. 2010. Fast signals and slow marks: the dynamics of histone modifications. *Trends Biochem. Sci.* 35:618–626. http://dx.doi.org/10.1016/j.tibs.2010.05.006

Basch, M.L., M. Bronner-Fraser, and M.I. García-Castro. 2006. Specification of the neural crest occurs during gastrulation and requires Pax7. *Nature.* 441:218–222. http://dx.doi.org/10.1038/nature04684

Beckmann, J.F., T.W. Markowski, B.A. Witthuhn, and A.M. Fallon. 2013. Detection of the Wolbachia-encoded DNA binding protein, HU beta, in mosquito gonads. *Insect Biochem. Mol. Biol.* 43:272–279. http://dx.doi.org/10.1016/j.ibmb.2012.12.007

Berndt, J.D., M.R. Clay, T. Langenberg, and M.C. Halloran. 2008. Rho-kinase and myosin II affect dynamic neural crest cell behaviors during epithelial to mesenchymal transition in vivo. *Dev. Biol.* 324:236–244. http://dx.doi.org/10.1016/j.ydbio.2008.09.013

Boulter, E., S. Estrach, R. Garcia-Mata, and C.C. Féral. 2012. Off the beaten paths: alternative and crosstalk regulation of Rho GTPases. *FASEB J.* 26:469–479. http://dx.doi.org/10.1096/fj.11-192252

Bronner-Fraser, M., and M. García-Castro. 2008. Manipulations of neural crest cells or their migratory pathways. *Methods Cell Biol.* 87:75–96. http://dx.doi.org/10.1016/S0091-679X(08)00204-5

Carmona-Fontaine, C., E. Theveneau, A. Tzekou, M. Tada, M. Woods, K.M. Page, M. Parsons, J.D. Lambris, and R. Mayor. 2011. Complement fragment C3a controls mutual cell attraction during collective cell migration. *Dev. Cell.* 21:1026–1037. http://dx.doi.org/10.1016/j.devcel.2011.10.012

Cavallius, J., W. Zoll, K. Chakraburtty, and W.C. Merrick. 1993. Characterization of yeast EF-1 alpha: non-conservation of post-translational modifications. *Biochim. Biophys. Acta.* 1163:75–80. http://dx.doi.org/10.1016/0167-4838(93)90281-U

Cavallius, J., A.P. Popkie, and W.C. Merrick. 1997. Site-directed mutants of post-translationally modified sites of yeast eEF1A using a shuttle vector containing a chromogenic switch. *Biochim. Biophys. Acta.* 1350:345–358. http://dx.doi.org/10.1016/S0167-4781(96)00181-9

Cheng, Y., M. Cheung, M.M. Abu-Elmagd, A. Orme, and P.J. Scotting. 2000. Chick sox10, a transcription factor expressed in both early neural crest cells and central nervous system. *Brain Res. Dev. Brain Res.* 121:233–241. http://dx.doi.org/10.1016/S0165-3806(00)00049-3

Chiang, P.K., R.K. Gordon, J. Tal, G.C. Zeng, B.P. Doctor, K. Pardhasaradhi, and P.P. McCann. 1996. S-Adenosylmethionine and methylation. *FASEB J.* 10:471–480.

Cho, H.S., T. Shimazu, G. Toyokawa, Y. Daigo, Y. Maehara, S. Hayami, A. Ito, K. Masuda, N. Ikawa, H.I. Field, et al. 2012. Enhanced HSP70 lysine methylation promotes proliferation of cancer cells through activation of Aurora kinase B. *Nat Commun.* 3:1072. http://dx.doi.org/10.1038/ncomms2074

Chuikov, S., J.K. Kurash, J.R. Wilson, B. Xiao, N. Justin, G.S. Ivanov, K. McKinney, P. Tempst, C. Prives, S.J. Gamblin, et al. 2004. Regulation of p53 activity through lysine methylation. *Nature.* 432:353–360. http://dx.doi.org/10.1038/nature03117

Clay, M.R., and M.C. Halloran. 2011. Regulation of cell adhesions and motility during initiation of neural crest migration. *Curr. Opin. Neurobiol.* 21:17–22. http://dx.doi.org/10.1016/j.conb.2010.09.013

Collings, D.A., G.O. Wasteneys, M. Miyazaki, and R.E. Williamson. 1994. Elongation factor 1 alpha is a component of the subcortical actin bundles of characean algae. *Cell Biol. Int.* 18:1019–1024. http://dx.doi.org/10.1006/cbir.1994.1025

Condeelis, J., and R.H. Singer. 2005. How and why does beta-actin mRNA target? *Biol. Cell.* 97:97–110. http://dx.doi.org/10.1042/BC20040063

Couttas, T.A., M.J. Raftery, M.P. Padula, B.R. Herbert, and M.R. Wilkins. 2012. Methylation of translation-associated proteins in Saccharomyces cerevisiae: Identification of methylated lysines and their methyltransferases. *Proteomics.* 12:960–972. http://dx.doi.org/10.1002/pmic.201100570

De Calisto, J., C. Araya, L. Marchant, C.F. Riaz, and R. Mayor. 2005. Essential role of non-canonical Wnt signalling in neural crest migration. *Development.* 132:2587–2597. http://dx.doi.org/10.1242/dev.01857

Dever, T.E., C.E. Costello, C.L. Owens, T.L. Rosenberry, and W.C. Merrick. 1989. Location of seven post-translational modifications in rabbit elongation factor 1 alpha including dimethyllysine, trimethyllysine, and glycerylphosphorylethanolamine. *J. Biol. Chem.* 264:20518–20525.

Dharmawardhane, S., M. Demma, F. Yang, and J. Condeelis. 1991. Compartmentalization and actin binding properties of ABP-50: the elongation factor-1 alpha of *Dictyostelium. Cell Motil. Cytoskeleton.* 20:279–288. http://dx.doi.org/10.1002/cm.970200404

Dricu, E. 2012 Methylation: From DNA, RNA and Histones to Diseases and Treatment. E. Dricu, editor. InTech. Rijeka, Croatia. 301 pp.

Edmonds, B.T., J. Murray, and J. Condeelis. 1995. pH regulation of the F-actin binding properties of *Dictyostelium* elongation factor 1 alpha. *J. Biol. Chem.* 270:15222–15230. http://dx.doi.org/10.1074/jbc.270.25.15222

Etchevers, H. 2011. Primary culture of chick, mouse or human neural crest cells. *Nat. Protoc.* 6:1568–1577. http://dx.doi.org/10.1038/nprot.2011.398

Fabianowska-Majewska, K., J.A. Duley, and H.A. Simmonds. 1994. Effects of novel adenosine analogues on the activity of S-adenosylhomocysteine hydrolase from human liver. *Biochem. Pharmacol.* 48:897–903. http://dx.doi.org/10.1016/0006-2952(94)90360-3

Gammill, L.S., and M. Bronner-Fraser. 2002. Genomic analysis of neural crest induction. *Development.* 129:5731–5741. http://dx.doi.org/10.1242/dev.00175

Gammill, L.S., and C.E. Krull. 2011. Embryological and genetic manipulation of chick development. *Methods Mol. Biol.* 770:119–137. http://dx.doi.org/10.1007/978-1-61779-210-6_5

Gao, D., Z. Li, T. Murphy, and W. Sauerbier. 1997. Structure and transcription of the gene for translation elongation factor 1 subunit alpha of zebrafish (Danio rerio). *Biochim. Biophys. Acta.* 1350:1–5. http://dx.doi.org/10.1016/S0167-4781(96)00179-0

Guendel, I., L. Carpio, C. Pedati, A. Schwartz, C. Teal, F. Kashanchi, and K. Kehn-Hall. 2010. Methylation of the tumor suppressor protein, BRCA1, influences its transcriptional cofactor function. *PLoS ONE.* 5:e11379. http://dx.doi.org/10.1371/journal.pone.0011379

Guerrier, S., J. Coutinho-Budd, T. Sassa, A. Gresset, N.V. Jordan, K. Chen, W.L. Jin, A. Frost, and F. Polleux. 2009. The F-BAR domain of srGAP2 induces membrane protrusions required for neuronal migration and morphogenesis. *Cell.* 138:990–1004. http://dx.doi.org/10.1016/j.cell.2009.06.047

Guo, S., and S. Bao. 2010. srGAP2 arginine methylation regulates cell migration and cell spreading through promoting dimerization. *J. Biol. Chem.* 285:35133–35141. http://dx.doi.org/10.1074/jbc.M110.153429

Hamburger, V., and H.L. Hamilton. 1992. A series of normal stages in the development of the chick embryo. 1951. *Dev. Dyn.* 195:231–272. http://dx.doi.org/10.1002/aja.1001950404

Heaslip, A.T., M. Nishi, B. Stein, and K. Hu. 2011. The motility of a human parasite, *Toxoplasma gondii,* is regulated by a novel lysine methyltransferase. *PLoS Pathog.* 7:e1002201. http://dx.doi.org/10.1371/journal.ppat.1002201

Hershfield, M.S., and N.M. Krodich. 1978. S-adenosylhomocysteine hydrolase is an adenosine-binding protein: a target for adenosine toxicity. *Science.* 202:757–760. http://dx.doi.org/10.1126/science.715439

Hiatt, W.R., R. Garcia, W.C. Merrick, and P.S. Sypherd. 1982. Methylation of elongation factor 1 alpha from the fungus Mucor. *Proc. Natl. Acad. Sci. USA.* 79:3433–3437. http://dx.doi.org/10.1073/pnas.79.11.3433

Hu, N., P. Strobl-Mazzulla, T. Sauka-Spengler, and M.E. Bronner. 2012. DNA methyltransferase3A as a molecular switch mediating the neural tube-to-neural crest fate transition. *Genes Dev.* 26:2380–2385. http://dx.doi.org/10.1101/gad.198747.112

Huang, J., and S.L. Berger. 2008. The emerging field of dynamic lysine methylation of non-histone proteins. *Curr. Opin. Genet. Dev.* 18:152–158. http://dx.doi.org/10.1016/j.gde.2008.01.012

Huq, M.D., S.G. Ha, H. Barcelona, and L.N. Wei. 2009. Lysine methylation of nuclear co-repressor receptor interacting protein 140. *J. Proteome Res.* 8:1156–1167. http://dx.doi.org/10.1021/pr800569c

Iwabata, H., M. Yoshida, and Y. Komatsu. 2005. Proteomic analysis of organ-specific post-translational lysine-acetylation and -methylation in mice by use of anti-acetyllysine and -methyllysine mouse monoclonal antibodies. *Proteomics.* 5:4653–4664. http://dx.doi.org/10.1002/pmic.200500042

Kernstock, S., E. Davydova, M. Jakobsson, A. Moen, S. Pettersen, G.M. Mælandsmo, W. Egge-Jacobsen, and P.O. Falnes. 2012. Lysine methylation of VCP by a member of a novel human protein methyltransferase family. *Nat Commun.* 3:1038. http://dx.doi.org/10.1038/ncomms2041

Kislauskis, E.H., X. Zhu, and R.H. Singer. 1994. Sequences responsible for intracellular localization of beta-actin messenger RNA also affect cell phenotype. *J. Cell Biol.* 127:441–451. http://dx.doi.org/10.1083/jcb.127.2.441

Kislauskis, E.H., X. Zhu, and R.H. Singer. 1997. beta-Actin messenger RNA localization and protein synthesis augment cell motility. *J. Cell Biol.* 136:1263–1270. http://dx.doi.org/10.1083/jcb.136.6.1263

Kozlowska, M., R.T. Smolenski, W. Makarewicz, C. Hoffmann, B. Jastorff, and J. Swierczynski. 1999. ATP depletion, purine riboside triphosphate accumulation and rat thymocyte death induced by purine riboside. *Toxicol. Lett.* 104:171–181. http://dx.doi.org/10.1016/S0378-4274(98)00369-5

Kulesa, P.M., and S.E. Fraser. 2000. In ovo time-lapse analysis of chick hindbrain neural crest cell migration shows cell interactions during migration to the branchial arches. *Development.* 127:1161–1172.

Kulesa, P.M., and L.S. Gammill. 2010. Neural crest migration: patterns, phases and signals. *Dev. Biol.* 344:566–568. http://dx.doi.org/10.1016/j.ydbio.2010.05.005

Lee, S., A.C. Doxey, B.J. McConkey, and B.A. Moffatt. 2012. Nuclear targeting of methyl-recycling enzymes in Arabidopsis thaliana is mediated by specific protein interactions. *Mol. Plant.* 5:231–248. http://dx.doi.org/10.1093/mp/ssr083

Lee, V.M., and P.Y. Lwigale. 2008. Neural crest, sensory neuron, and muscle cultures. *Methods Cell Biol.* 87:115–133. http://dx.doi.org/10.1016/S0091-679X(08)00206-9

Levy, D., C.L. Liu, Z. Yang, A.M. Newman, A.A. Alizadeh, P.J. Utz, and O. Gozani. 2011. A proteomic approach for the identification of novel lysine methyltransferase substrates. *Epigenetics Chromatin.* 4:19. http://dx.doi.org/10.1186/1756-8935-4-19

Lin-Moshier, Y., P.J. Sebastian, L. Higgins, N.D. Sampson, J.E. Hewitt, and J.S. Marchant. 2013. Re-evaluation of the role of calcium homeostasis endoplasmic reticulum protein (CHERP) in cellular calcium signaling. *J. Biol. Chem.* 288:355–367. http://dx.doi.org/10.1074/jbc.M112.405761

Lipson, R.S., K.J. Webb, and S.G. Clarke. 2010. Two novel methyltransferases acting upon eukaryotic elongation factor 1A in Saccharomyces cerevisiae. *Arch. Biochem. Biophys.* 500:137–143. http://dx.doi.org/10.1016/j.abb.2010.05.023

Liu, G., W.M. Grant, D. Persky, V.M. Latham Jr., R.H. Singer, and J. Condeelis. 2002. Interactions of elongation factor 1alpha with F-actin and beta-actin mRNA: implications for anchoring mRNA in cell protrusions. *Mol. Biol. Cell.* 13:579–592. http://dx.doi.org/10.1091/mbc.01-03-0140

Magrane, M., and U. Consortium. 2011. UniProt Knowledgebase: a hub of integrated protein data. *Database (Oxford).* 2011:bar009.

Matthews, H.K., L. Marchant, C. Carmona-Fontaine, S. Kuriyama, J. Larraín, M.R. Holt, M. Parsons, and R. Mayor. 2008. Directional migration of neural crest cells in vivo is regulated by Syndecan-4/Rac1 and non-canonical Wnt signaling/RhoA. *Development.* 135:1771–1780. http://dx.doi.org/10.1242/dev.017350

Moore, K.E., S.M. Carlson, N.D. Camp, P. Cheung, R.G. James, K.F. Chua, A. Wolf-Yadlin, and O. Gozani. 2013. A general molecular affinity strategy for global detection and proteomic analysis of lysine methylation. *Mol. Cell.* 50:444–456. http://dx.doi.org/10.1016/j.molcel.2013.03.005

Murray, J.W., B.T. Edmonds, G. Liu, and J. Condeelis. 1996. Bundling of actin filaments by elongation factor 1 alpha inhibits polymerization at filament ends. *J. Cell Biol.* 135:1309–1321. http://dx.doi.org/10.1083/jcb.135.5.1309

Ong, S.E., G. Mittler, and M. Mann. 2004. Identifying and quantifying in vivo methylation sites by heavy methyl SILAC. *Nat. Methods.* 1:119–126. http://dx.doi.org/10.1038/nmeth715

Pang, C.N., E. Gasteiger, and M.R. Wilkins. 2010. Identification of arginine- and lysine-methylation in the proteome of Saccharomyces cerevisiae and its functional implications. *BMC Genomics.* 11:92. http://dx.doi.org/10.1186/1471-2164-11-92

Polevoda, B., and F. Sherman. 2007. Methylation of proteins involved in translation. *Mol. Microbiol.* 65:590–606. http://dx.doi.org/10.1111/j.1365-2958.2007.05831.x

Prasad, M.S., T. Sauka-Spengler, and C. LaBonne. 2012. Induction of the neural crest state: control of stem cell attributes by gene regulatory, post-transcriptional and epigenetic interactions. *Dev. Biol.* 366:10–21. http://dx.doi.org/10.1016/j.ydbio.2012.03.014

R Development Core Team. 2011. R: A Language and Environment for Statistical Computing. Vienna, Austria: R Foundation for Statistical Computing. Retrieved from http://www.R-project.org.

Radomski, N., C. Kaufmann, and C. Dreyer. 1999. Nuclear accumulation of S-adenosylhomocysteine hydrolase in transcriptionally active cells during development of *Xenopus laevis*. *Mol. Biol. Cell.* 10:4283–4298. http://dx.doi.org/10.1091/mbc.10.12.4283

Radomski, N., G. Barreto, C. Kaufmann, J. Yokoska, K. Mizumoto, and C. Dreyer. 2002. Interaction of S-adenosylhomocysteine hydrolase of Xenopus laevis with mRNA(guanine-7-)methyltransferase: implication on its nuclear compartmentalisation and on cap methylation of hnRNA. *Biochim. Biophys. Acta.* 1590:93–102. http://dx.doi.org/10.1016/S0167-4889(02)00205-7

Rappsilber, J., Y. Ishihama, and M. Mann. 2003. Stop and go extraction tips for matrix-assisted laser desorption/ionization, nanoelectrospray, and LC/MS sample pretreatment in proteomics. *Anal. Chem.* 75:663–670. http://dx.doi.org/10.1021/ac026117i

Riis, B., S.I. Rattan, B.F. Clark, and W.C. Merrick. 1990. Eukaryotic protein elongation factors. *Trends Biochem. Sci.* 15:420–424. http://dx.doi.org/10.1016/0968-0004(90)90279-K

Roffers-Agarwal, J., K.J. Hutt, and L.S. Gammill. 2012. Paladin is an antiphosphatase that regulates neural crest cell formation and migration. *Dev. Biol.* 371:180–190. http://dx.doi.org/10.1016/j.ydbio.2012.08.007

Rottner, K., and T.E. Stradal. 2011. Actin dynamics and turnover in cell motility. *Curr. Opin. Cell Biol.* 23:569–578. http://dx.doi.org/10.1016/j.ceb.2011.07.003

Schaefer, A., M. Nethe, and P.L. Hordijk. 2012. Ubiquitin links to cytoskeletal dynamics, cell adhesion and migration. *Biochem. J.* 442:13–25. http://dx.doi.org/10.1042/BJ20111815

Schneider, C.A., W.S. Rasband, and K.W. Eliceiri. 2012. NIH Image to ImageJ: 25 years of image analysis. *Nat. Methods.* 9:671–675. http://dx.doi.org/10.1038/nmeth.2089

Sherman, M., and P.S. Sypherd. 1989. Role of lysine methylation in the activities of elongation factor 1 alpha. *Arch. Biochem. Biophys.* 275:371–378. http://dx.doi.org/10.1016/0003-9861(89)90384-6

Shevchenko, A., M. Wilm, O. Vorm, and M. Mann. 1996. Mass spectrometric sequencing of proteins silver-stained polyacrylamide gels. *Anal. Chem.* 68:850–858. http://dx.doi.org/10.1021/ac950914h

Shu, S., D.C. Mahadeo, X. Liu, W. Liu, C.A. Parent, and E.D. Korn. 2006. S-adenosylhomocysteine hydrolase is localized at the front of chemotaxing cells, suggesting a role for transmethylation during migration. *Proc. Natl. Acad. Sci. USA.* 103:19788–19793. http://dx.doi.org/10.1073/pnas.0609385103

Sinha, R., E. Allemand, Z. Zhang, R. Karni, M.P. Myers, and A.R. Krainer. 2010. Arginine methylation controls the subcellular localization and functions of the oncoprotein splicing factor SF2/ASF. *Mol. Cell. Biol.* 30:2762–2774. http://dx.doi.org/10.1128/MCB.01270-09

Slobin, L.I. 1980. The role of eucaryotic factor Tu in protein synthesis. The measurement of the elongation factor Tu content of rabbit reticulocytes and other mammalian cells by a sensitive radioimmunoassay. *Eur. J. Biochem.* 110:555–563. http://dx.doi.org/10.1111/j.1432-1033.1980.tb04898.x

Strobl-Mazzulla, P.H., T. Sauka-Spengler, and M. Bronner-Fraser. 2010. Histone demethylase JmjD2A regulates neural crest specification. *Dev. Cell.* 19:460–468. http://dx.doi.org/10.1016/j.devcel.2010.08.009

Su, I.H., M.W. Dobenecker, E. Dickinson, M. Oser, A. Basavaraj, R. Marqueron, A. Viale, D. Reinberg, C. Wülfing, and A. Tarakhovsky. 2005. Polycomb group protein ezh2 controls actin polymerization and cell signaling. *Cell.* 121:425–436. http://dx.doi.org/10.1016/j.cell.2005.02.029

Swartz, M., J. Eberhart, G.S. Mastick, and C.E. Krull. 2001. Sparking new frontiers: using in vivo electroporation for genetic manipulations. *Dev. Biol.* 233:13–21. http://dx.doi.org/10.1006/dbio.2001.0181

Teddy, J.M., and P.M. Kulesa. 2004. In vivo evidence for short- and long-range cell communication in cranial neural crest cells. *Development.* 131:6141–6151. http://dx.doi.org/10.1242/dev.01534

Theveneau, E., and R. Mayor. 2010. Integrating chemotaxis and contact-inhibition during collective cell migration: Small GTPases at work. *Small GTPases.* 1:113–117. http://dx.doi.org/10.4161/sgtp.1.2.13673

Theveneau, E., and R. Mayor. 2012. Neural crest delamination and migration: from epithelium-to-mesenchyme transition to collective cell migration. *Dev. Biol.* 366:34–54. http://dx.doi.org/10.1016/j.ydbio.2011.12.041

Ueland, P.M., and S. Helland. 1983. Binding of adenosine to intracellular S-adenosylhomocysteine hydrolase in isolated rat hepatocytes. *J. Biol. Chem.* 258:747–752.

Vermillion, K.L., K. Lidberg, and L.S. Gammill. 2013. Expression of actin-binding proteins and requirement for actin depolymerizing factor in chick neural crest cells. *Dev. Dyn.* In press.

Vladimirov, N., and V. Sourjik. 2009. Chemotaxis: how bacteria use memory. *Biol. Chem.* 390:1097–1104.

Wilkinson, D.G. 1992. *In Situ* Hybridization: A Practical Approach. IRL Press, Oxford, England. 224 pp.

Xiao, H., K. El Bissati, P. Verdier-Pinard, B. Burd, H. Zhang, K. Kim, A. Fiser, R.H. Angeletti, and L.M. Weiss. 2010. Post-translational modifications to *Toxoplasma gondii* alpha- and beta-tubulins include novel C-terminal methylation. *J. Proteome Res.* 9:359–372. http://dx.doi.org/10.1021/pr900699a

Young, N.L., P.A. DiMaggio, and B.A. Garcia. 2010. The significance, development and progress of high-throughput combinatorial histone code analysis. *Cell. Mol. Life Sci.* 67:3983–4000. http://dx.doi.org/10.1007/s00018-010-0475-7

Zhang, X., H. Wen, and X. Shi. 2012. Lysine methylation: beyond histones. *Acta Biochim. Biophys. Sin. (Shanghai).* 44:14–27. http://dx.doi.org/10.1093/abbs/gmr100

Zhang, Y., T.H. Kim, and L. Niswander. 2012. Phactr4 regulates directional migration of enteric neural crest through PP1, integrin signaling, and cofilin activity. *Genes Dev.* 26:69–81. http://dx.doi.org/10.1101/gad.179283.111